Check for updates

Screening the deep eutectic electrolytes for supercapacitors with alleviated self-discharge†

Wenxia Huang, Xiaohui Yan, Yige Xiong, Qihui Guo, Xin Zhang, Fengyu Huang, Houqiang Shi and Xiang Ge 🔴 *

Self-discharge in supercapacitors is a major challenge and it's mainly determined by the property of the electrolyte. The emergence of deep eutectic solvents (DESs) provides a promising research frontier, but the principle of selecting DESs with suppressed self-discharge is not well understood. Herein, we prepared various DESs with the same hydrogen bond acceptor (HBA) but different hydrogen bond donors (HBDs) to unveil the effect of the type and number of functional groups in the HBD on the self-discharge property in symmetric supercapacitors. In acidic DESs (where the HBD has carboxyl −COOH groups or is acidic), a higher number of carboxyl groups are detrimental for self-discharge. For alkaline DESs (where the HBD has amino −NH$_2$ groups), a higher number of amino groups are also disadvantageous for self-discharge. Conversely, in neutral DESs (where the HBD has neither −COOH nor −NH$_2$ groups, and it do not exhibit acidity either), a higher number of hydroxyl groups is favorable for alleviating self-discharge. The supercapacitors using ChCl:Gly electrolyte exhibit the highest capability for alleviating self-discharge (32% voltage retention rate when aged for 15 h). The influence of harsh reaction conditions (temperature and water impurity) was also studied for the ChCl:Gly electrolyte. These results are expected to guide the further optimization of electrolytes with suppressed self-discharge.

1. Introduction

High-performance energy storage technologies are key elements for the rising energy crisis.[1–9] Compared to traditional batteries, supercapacitors show many advantages such as high-power densities and excellent cycling stability.[10–13] Nevertheless, self-discharge has placed severe limitations on the wider applications of electrochemical double layer capacitors (EDLCs).[12,14,15] Self-discharge describes the phenomenon that for the charged device, the adsorbed charge carriers would spontaneously diffuse away from the electrode/electrolyte interface and diffuse into the electrolyte, resulting in the loss of stored energy.[16–18] To suppress self-discharge, the optimization of the electrolyte is one of the most effective approaches.[19,20] Currently, electrolytes used in supercapacitors are generally classified into three types: aqueous, organic and ionic liquid.[20–23] Each system has its pros and cons in terms of the various properties including energy density, cost, life span, rate capability, *etc.*[24,25] Tremendous efforts have been devoted to optimizing one of the properties selectively by using the most suitable electrolytes.[26–29] However, the suppression of self-discharge is still unsatisfactory using currently known electrolytes, thus calling for a search for novel electrolytes.

Deep eutectic solvents (DESs), reported by Abbott and coworkers in 2003,[30] are generally formed by directly mixing hydrogen bond acceptor (HBA) and hydrogen bond donor (HBD) species.[31] DESs are eutectic mixtures with a melting point far below that of individual components due to the charge delocalization occurring through hydrogen bonding between the HBA and HBD.[30,32] Compared with traditional electrolytes mentioned above, DESs have many advantages such as lower price, better safety, and environmental friendliness.[33–38] Noteworthily, the partially ionic structure of DESs renders them with moderate mobility of ions. As the formation of DESs is accompanied by the combination of various types of HBAs and HBDs, theoretically, there exist plenty of different types of DESs (more than 10^6), among which the DESs based on choline chloride (ChCl, used as HBA) have received the most attention due to their low cost and easy preparation for various applications.[39–42] Unfortunately, how to select DESs as electrolytes with suppressed self-discharge is largely unknown.

Herein, we prepared a series of DESs using various kinds of HBD species to explore how the structure would determine the self-discharge process of symmetric supercapacitors. With the systematic characterization of the electrolyte and comparison of the electrochemical performance, it's concluded that the

Department of Materials and Metallurgy, Guizhou University, Guiyang, Guizhou 550025, China. E-mail: xge@gzu.edu.cn

functional groups of the HBD species have a significant influence on the self-discharge performance. For acidic DESs (HBD has carboxyl –COOH groups or is acidic), a higher number of carboxyl groups (–COOH) would be detrimental for self-discharge. For alkaline DESs (HBD has amino –NH$_2$ groups), a higher number of the amino –NH$_2$ is disadvantageous for self-discharge. For neutral DESs (the HBD has no –COOH nor –NH$_2$, and it do not exhibit acidity either), a higher number of the hydroxyl groups would be favorable for alleviating self-discharge. This result indicates that the structure of the HBD has a profound and complex influence on the self-discharge process. During the selection of the electrolyte by focusing on the functional groups of the composing raw materials, the type of DESs should be first considered. This work is expected to serve as preliminary guidance for the optimization of the electrolytes in supercapacitors.

2. Experimental section

2.1 Synthesis procedure for DES-based electrolytes

Various types of DESs were prepared by mixing HBDs and the HBA with a molar ratio of 1:2. The studied HBD species include phenol (≥99.0%, Chengshi), oxalic acid (98%, Energy Chemical), malonic acid (98%, Energy Chemical), levulinic acid (98%, Energy Chemical), acetamide (98%, Energy Chemical), ethylene glycol (98%, Energy Chemical), glycerol (99%, Energy Chemical) and urea (99%, Energy Chemical), respectively, while choline chloride (ChCl) (>98%, Energy Chemical) was used as the HBA. Then eight kinds of transparent DESs were obtained by heating the mixtures at 70 °C for 60 mins. The liquids with different HBDs (phenol, oxalic acid, malonic acid, levulinic acid, acetamide, ethylene glycol, glycerol and urea) were named ChCl:Phenol, ChCl:OA, ChCl:MA, ChCl:LA, ChCl:Ace, ChCl:EG, ChCl:Gly, and ChCl:Urea, respectively.

2.2 Assembly of symmetric supercapacitors based on DES electrolytes

The working electrodes were obtained *via* a slurry-coating method. The active carbon (AC) was used as the active material. The slurry was formed by mixing the active materials, the conductive carbon and the PVDF binder with a weight ratio of 8:1:1. Then, the working electrodes were obtained by loading the slurry on the nickel foam current collector with a diameter of 12 mm. After being dried at 110 °C under vacuum for 12 h, the electrodes were then flattened by a tablet press. For evaluating the electrochemical performance, symmetric supercapacitors were assembled using CR2032 coin cells. Pairs of AC electrodes were used as the electrodes. Polypropylene was used as the separator. The prepared DESs were used as the electrolytes.

2.3 Material characterization and electrochemical measurement

The characterization of the porous structure and morphology for the AC was conducted by an automated surface area and porosity analyzer (BET, ASAP 2460), a scanning electron microscope (SEM, HITACHI-SU8010) and a transmission electron microscope (TEM, Tecnai G2 F20 at 200 kV). The molecular structure of the DESs was examined by Fourier transform infrared (FTIR, Thermo Scientific Nicolet iS20). For electrochemical characterization, all the assembled batteries were aged for 5 h before measurements. Cyclic voltammetry (CV) was tested using a CHI660e electrochemical workstation (Chenhua, Shanghai). The self-discharge and cycling stability were tested on a LAND battery program-control test system.

3. Results and discussion

3.1 Working mechanism of DES-based electrolytes

Self-discharge has seriously impeded the widespread use of EDLCs.[15] It refers to the spontaneous migration of charge carriers from the electrode material into the electrolyte. Electrolytes play the key role for the self-discharge process of supercapacitors.[20] In recent years, a diverse range of DESs have yielded promising chances to meet specific requirements in terms of their properties.[43] Based on the composition, DESs are typically divided into four categories: Cat^+X^- $zMCl_x$ (where z is the number of MCl_x molecules that interact with the anion and M is Zn, Sn, Fe, Al, Ga, or In); Cat^+X^- $zMCl_x \cdot yH_2O$ (where M is Cr, Co, Cu, Ni, or Fe); Cat^+X^- zRZ (where Z is $CONH_2$, COOH, or OH and R is the general formula of hydrocarbon groups or alkyl groups); and $MCl_x + RZ = MCl_{x-1}^+ \cdot RZ + MCl_{x+1}^-$ (where M is Al or Zn and Z is $CONH_2$ or OH).[44] Currently, extensive research effort has been focused on Cat^+X^- zRZ Type DESs (using ChCl as the Cat^+X^-) in various applications due to their low cost, easy preparation and environmental friendliness.[45] The exploration of this type of DES as electrolytes for supercapacitors is thus desirable. In order to understand the impact of the structure of electrolytes on self-discharge in symmetric supercapacitors, this work uses eight types of HBDs while ChCl was used as the HBA specie to form DESs (as depicted in Fig. 1a) and we studied their performances.

To gain insights into the correlation between the structure of DESs and the self-discharge behavior for supercapacitors, the migration of the species in the prepared electrolyte was analyzed. Fig. 1b schematically illustrates the AC/AC supercapacitor working with the ChCl:Gly type electrolytes. During charging, the ions inside the electrolyte migrate towards their corresponding electrode/electrolyte interfaces for the device to store energy: the cations move towards the anode while the anions move towards the cathode.[46,47] The characteristic of the electrolyte could determine the self-discharge process based on two mechanisms. On one hand, at the electrode/electrolyte interface, the AC electrodes provide a large surface area for the electrolyte ions to interact with, leading to the formation of an electric double layer.[48] Therefore, the interaction between electrolyte ions and electrodes is crucial for improving the performance and stability of energy storage devices. On the other hand, the bulk property of the electrolytes could also influence the migration of ions.[49] Consequently, the specific functional groups in the HBD species for forming the hydrogen bonds in the eutectic electrolytes, such as hydroxyl groups (–OH), could play a critical role in the
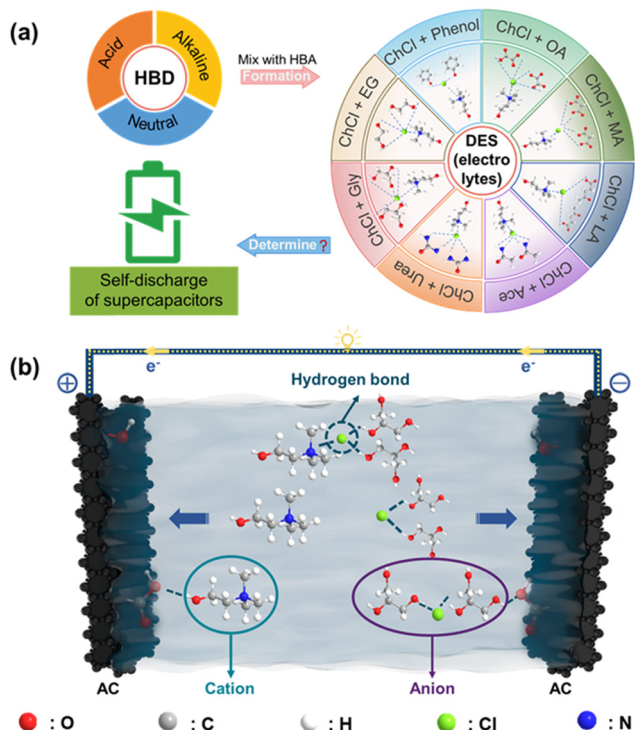
Fig. 1 Schematic illustration showing that the structure of the electrolyte could have a profound influence on the self-discharge process of super-capacitors. (a) The superstructure of DESs can be tuned by combining various types of HBA and HBD species, thus providing an ideal research platform. (b) The working principle of the symmetric supercapacitor based on ChCl:Gly electrolyte with AC as the electrode material.

electrochemical performance of supercapacitors.[23,47] Therefore, examining the functional groups could be an effective strategy for screening the HBD species in the DESs, and is expected to be critical for designing high-performance eutectic electrolytes.

3.2 Structure characterization and transport properties

As discussed above, hydrogen bonds play a significant role in shaping the structures of DESs. The spectral feature of the hydrogen bonds can be categorized into two classes. The first class is the red-shift hydrogen bonds,[50] and the second type is the blue-shift hydrogen bonds.[51,52] FTIR spectroscopy (Fig. 2) was utilized to study the prepared DESs. In general, the wavenumber in FTIR spectroscopy is directly proportional to the frequency of the molecular vibration responsible for the peak. For X–H bonds, such as O–H, the frequency of the stretching vibration is inversely proportional to the square root of the bond length. Therefore, a red-shift hydrogen bond indicates a longer X–H bond length, resulting in a lower stretching frequency and a shift towards shorter wavenumbers. In contrast, a blue-shift hydrogen bond indicates a weaker bond and a shorter X–H bond length, resulting in a higher stretching frequency and a shift towards longer wavenumbers. On the basis of the analysis of the spectroscopy,[53] we first compared the signal of pristine EG and Gly (neither of them has –COOH or –NH$_2$ functional groups), as well as the DESs synthesized from them. The FTIR spectra (Fig. 2) reveal the
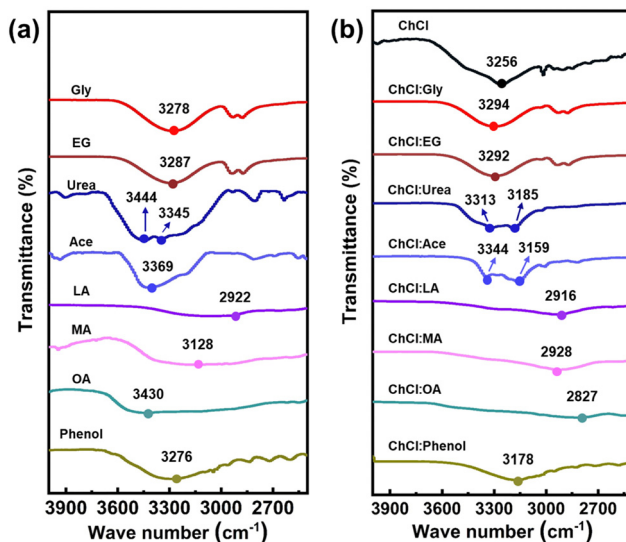
Fig. 2 FTIR spectra of the DESs tested in the range of 4000–2500 cm^{-1}. (a) FTIR spectra for the 8 pristine HBDs. (b) FTIR spectra of the pristine ChCl as the HBA and the corresponding DESs with the molar ratio of 1 HBA : 2 HBD.

presence of peaks at 3287 cm^{-1}, 3278 cm^{-1}, 3292 and 3294 cm^{-1}, which correspond to the O–H stretching vibration of EG, Gly, ChCl:EG and ChCl:Gly, respectively. Compared to the O–H stretching vibration of pure EG or pure Gly, the FTIR spectra of the two corresponding DESs show a blue shift for their hydrogen bonds. This suggests that the hydrogen bonds in ChCl:EG and ChCl:Gly show decreased length. For acidic DESs (HBD has carboxyl –COOH groups or is acidic), a comparison of the O–H stretching vibration of ChCl:Phenol, ChCl:OA, ChCl:MA, and ChCl:LA, with that of the corresponding HBDss shows a red shift, indicating that the formation of the hydrogen bonding between the HBAs and HBDs results in increased O-H bond length. Then, the comparison of alkaline DESs (HBD has amino –NH$_2$ groups) was conducted. Visibly, peaks appearing at 3369 cm^{-1} and 3345 cm^{-1} (3444 cm^{-1}) could respectively represent –NH$_2$ stretching vibration peaks in Ace and Urea. In Fig. 2b, those peaks shift towards shorter wavenumbers (3159 cm^{-1}/ 3344 cm^{-1}, 3185 cm^{-1}/3313 cm^{-1}), suggesting the formation of red-shift hydrogen bonds. In conclusion, the results demonstrate the formation of hydrogen bonds in all DESs systems and indicate that various types of HBDs have different effects on intermolecular interactions and the superstructure of DESs.

The different structure of the DESs endows them with different properties. The viscosity, density and ionic conductivity are key parameters that determine the suitability of DESs for use in EDLCs. As shown in Table S1 (ESI†), the majority of DESs displayed relatively high viscosity (51–19 945 cP), moderate ionic conductivity (118–17 368 μS cm^{-1}) and a density slightly higher than water (1.007–1.358 g cm^{-3}). Besides, the structure of the used AC was characterized. In the XRD patterns (Fig. S1, ESI†), two broad peaks at ~21° and 44° indicate that the AC has relatively low crystallinity. In addition, the AC had a favorable porous surface structure (SEM, TEM in Fig. S2 (ESI†), N$_2$ adsorption/desorption profile and PSD curve derived from the DFT

Paper

method in Fig. S3, ESI†). After the structures of the electrolytes and the electrodes are clarified, they are then assembled to study the electrochemical performance.

3.3 The self-discharge and electrochemical performance of symmetric supercapacitors using DESs as electrolytes

In this study, we utilized eight types of DESs with the same HBA (ChCl) but various HBD species as electrolytes to assemble coin cells. We evaluated their self-discharge performance by measuring the change of the open circuit potential upon aging. The cells underwent stabilization by running 10 cycles and being kept at 1.0 V for 1.0 hour prior to testing. As shown in Fig. 3a, the voltage of all DESs decayed rapidly within the first two hours. The supercapacitor utilizing the ChCl:Gly electrolyte was significantly more stable in terms of self-discharge at the 15 hour mark. To reduce experimental error, we conducted multiple self-discharge tests, and we presented the residual voltages for supercapacitors based on various DESs in the form of bar charts to better visualize the self-discharge performance (Fig. 3b). The average residual

voltage of the supercapacitor utilizing ChCl:Gly was the highest, indicating that this electrolyte is the most suitable for alleviating self-discharge of supercapacitors. To further determine the electrochemical performance of various DES electrolytes, we conducted leakage current tests (Fig. 3c) and provided the corresponding enlarged views in Fig. 3d. During the first two hours of testing, the currents rapidly decayed as none of the cells had yet achieved stability, which is consistent with the voltage–time profile in Fig. 3a. Fig. 3e shows that in acidic DESs, a higher number of carboxyl (–COOH) groups led to a much lower voltage retention rate. A similar trend was observed for the amino (–NH$_2$) groups of alkaline DESs. Conversely, in neutral DESs, a higher number of hydroxyl groups were found to be favorable for alleviating self-discharge. Additionally, it is worth noting that the sensitivity of the three types of DESs to changes in the number of their respective functional groups varies. Specifically, alkaline electrolytes are less sensitive to changes in the number of the specific functional groups (–NH$_2$) than acidic electrolytes (–COOH). Building upon the two mechanisms discussed earlier
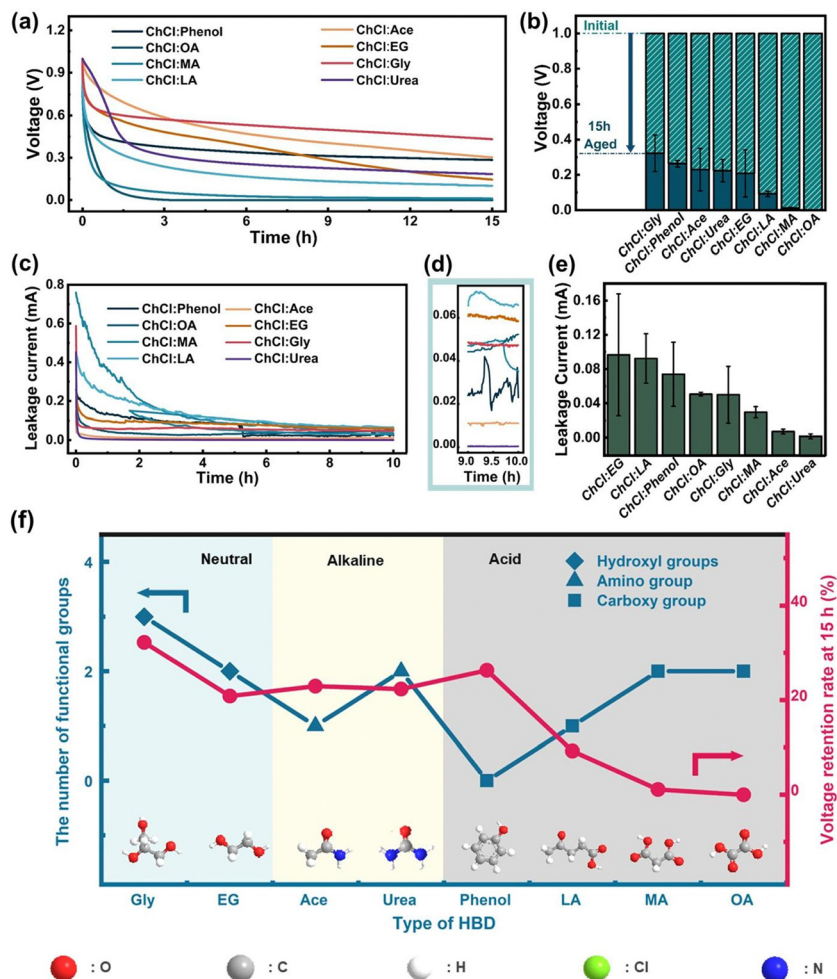
Fig. 3 The self-discharge and electrochemical performance of the symmetric supercapacitors with different DESs as electrolytes. (a) The voltage–time profile of the supercapacitors at open circuit conditions after charging. (b) The initial voltage and the retained voltage after an aging time of 900.0 min. (c) Leakage current curves of the supercapacitors at the constant voltage of 1 V. (d) The enlarged view of (c) at 9.0–10.0 h. (e) The average leakage current and error bar of the supercapacitors at 10 h. (f) The effect of the number and type of functional groups on the voltage retention rate of the DESs composed of different HBDs.

regarding the impact of electrolyte properties on the self-discharge process, we provide a more in-depth analysis of the aforementioned conclusions: an increased quantity of amino and carboxyl groups imparts a stronger alkaline or acidic nature to the DESs electrolyte, consequently affecting the interaction at the electrode interface and the rate of charge transfer, thus increasing the self-discharge rate of the supercapacitor. Simultaneously, the presence of hydroxyl groups improves the interaction between the electrolyte and the electrode interface, facilitating charge transfer and enhancing ion conductivity, thereby reducing the self-discharge rate of the supercapacitor. Thus, the type and quantity of functional groups significantly and intricately impact the self-discharge performance of supercapacitors.

3.4 The performance of ChCl:Gly at various water contents and temperatures

The impact of temperature is known to have a significant impact on the self-discharge process.[54] Additionally, the highly water-miscible and hygroscopic nature of DESs,[55] which is attributed to the coordination and hydrogen-bonding species within them, would usually involve water content, which would significantly influence their properties and structure.[56–58] In other words, water can act as both a hydrogen donor and a hydrogen acceptor, thereby competing with and disrupting the HBA:HBD hydrogen-bonding network in DESs,[59] which could potentially affect the self-discharge process. Therefore, it is imperative to investigate the impact of temperature and water content on the self-discharge behavior. The ChCl:Gly was selected as a representative electrolyte system for electrochemical tests due to its superior stability in terms of self-discharge. To investigate the influence of temperature, all assembled batteries were allowed to stand at the designated temperature for 10 h before collecting the data (also keeping at this temperature while measuring). Fig. 4a shows a gradual decrease in the retained voltage with increasing

temperature. Leakage current measurements in Fig. 4b also confirm that ChCl:Gly electrolyte at 24 °C has a higher ability in alleviating self-discharge than at 80 °C. An inflection point can be observed in Fig. 4b. The reason behind this experimental phenomenon may be traced back to the instability of the electrolyte caused by elevated temperatures. The leakage current test involves collecting the current magnitude under constant voltage conditions, and the test system may experience slight disturbances, leading to noticeable data fluctuations. Additionally, the volume characteristics of the electrolyte can also influence ion migration, thereby impacting the electrochemical performance of the supercapacitor. For the ChCl:Gly system with a molar ratio of 1:2 at 80 °C, the molecular kinetic energy of the solvent and solute increases, weakening the interactions between molecules, resulting in the expansion of the solution's volume. Gradual expansion of the electrolyte can exceed the capacity of the cell packaging, causing the inflection point observed in Fig. 4b. The influence of water content is given in Fig. 4c. Interestingly, the addition of a slight amount of water (1 vol%) resulted in the fastest self-discharge compared to pure ChCl:Gly (0 vol%) electrolyte or when the water content is higher (>3 vol%). The leakage current tests (Fig. 4d and z the zoomed-in view in Fig. 4e) are basically consistent with the voltage–time profile in Fig. 4c. Based on all results presented, higher temperature would lead to faster self-discharge while the influence of water is much more complex. The self-discharge phenomenon caused by higher temperature can be attributed to more intense movement of the electrolyte ions.[60] Additionally, the extensive hydrogen bond network between DES components will affect the mobility of free electrolyte ions within the system, which may further inhibit the self-discharge process to a certain extent. When water is introduced into the system, the hydrogen bonds between the DES components will be broken,[61,62] which would reduce the ability of the electrolyte to inhibit self-discharge.
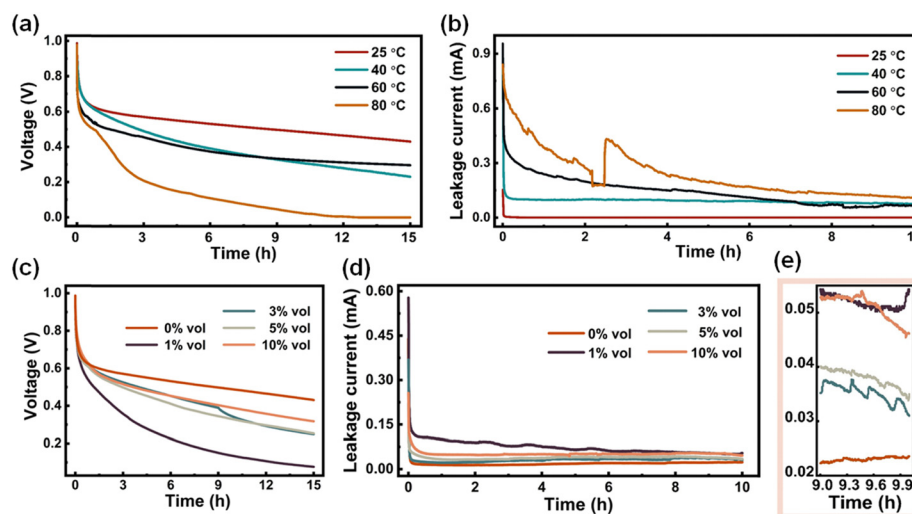

Fig. 4 The electrochemical performance of the symmetric supercapacitors using ChCl:Gly as electrolytes with the molar ratio of 1:2. (a) The voltage–time profile of the supercapacitors at open circuit conditions after charging, under different temperatures from 25 °C to 80 °C; (b) leakage current curves of the supercapacitors at the constant voltage of 1.0 V under different temperatures; (c) self-discharge performance when the electrolyte is added with given volumes of water; (d) leakage current curves with addition of various volumes of water. (e) The enlarged view of (d) at 9.0–10.0 h.

However, with the continuous addition of water, water molecules can effectively interact with each component, properly fit water molecules to the DES hydrogen bond network, and form new hydrogen bonds.[59,61] Still, the self-discharge of the supercapacitor using such aqueous electrolyte is still worse than that using pure DESs.

4. Conclusion

To explore how the structure of DES electrolytes would determine the self-discharge process of symmetric supercapacitors, we prepared eight types of DES-based supercapacitors with various HBD species. Through systematic characterization of the electrolytes and comparison of the electrochemical performance, we demonstrate that the self-discharge property is not simply determined by one specific physiochemical property of the electrolyte. Instead, the type and number of functional groups of the HBD could have a complex and significant effect on the superstructure of the DESs, ultimately impacting the self-discharge process. For designing DES electrolytes, the type (whether it has –COOH or NH_2 functional groups) of the studied DES should first be determined before selecting the number of functional groups. The reaction conditions (temperature of water impurity) are also important for self-discharge. These results are expected to guide for designing high-performance electrolytes with suppressed self-discharge.

Conflicts of interest

There are no conflicts to declare.

Acknowledgements

References

1 R. Raavi, S. Archana, P. Adinarayana Reddy and P. Elumalai, *Energy Adv.*, 2023, **2**, 385–397.
2 K. Prenger, Y. Sun, K. Ganeshan, A. Al-Temimy, K. Liang, C. Dun, J. J. Urban, J. Xiao, T. Petit, A. C. T. van Duin, D.-E. Jiang and M. Naguib, *ACS Appl. Energy Mater.*, 2022, **5**, 9373–9382.
3 A. Brady, K. Liang, V. Q. Vuong, R. Sacci, K. Prenger, M. Thompson, R. Matsumoto, P. Cummings, S. Irle, H.-W. Wang and M. Naguib, *ACS Nano*, 2021, **15**, 2994–3003.
4 S. Payá, N. Diez and M. Sevilla, *Sustainable Energy Fuels*, 2023, **7**, 2378–2389.
5 F. Wu, F. Chu, G. Ferrero, M. Sevilla, A. B. Fuertes, O. Borodin, Y. Yu and G. Yushin, *Nano Lett.*, 2020, **20**, 5391–5399.
6 X. Ge, S. Cao, Z. Lv, Z. Zhu, Y. Tang, H. Xia, H. Zhang, J. Wei, W. Zhang, Y. Zhang, Y. Zeng and X. Chen, *Adv. Mater.*, 2022, **34**, e2206797.
7 P. Simon and Y. Gogotsi, *Nat. Mater.*, 2020, **19**, 1151–1163.
8 X. Zhang, H. Shi, X. Yan, K. Liu, W. Huang, Q. Guo, F. Huang and X. Ge, *Energy Fuels*, 2022, **36**, 7140–7146.
9 Y. G. Xiong, X. H. Yan, T. B. Li, H. X. Jin, Z. L. Chen, X. J. Xu, X. Ji and X. Ge, *Chem. Eng. J.*, 2023, **451**, 138913.
10 S. Zallouz, J.-M. Le Meins and C. Matei Ghimbeu, *Energy Adv.*, 2022, **1**, 1051–1064.
11 Poonam, K. Sharma, A. Arora and S. K. Tripathi, *J. Energy Storage*, 2019, **21**, 801–825.
12 S. Jing, X. Yan, T. Li, Y. Xiong, T. Hu, Z. Wang and X. Ge, *J. Power Sources*, 2022, **549**, 232141.
13 Y. Wang and Y. Xia, *Adv. Mater.*, 2013, **25**, 5336–5342.
14 X. H. Yan, S. Q. Jing, T. B. Li, Y. G. Xiong, T. Hu, Z. J. Wang and X. Ge, *Chem. Eng. J.*, 2022, **450**, 137977.
15 W. Shang, W. Yu, X. Xiao, Y. Ma, Y. He, Z. Zhao and P. Tan, *Adv. Powder Technol.*, 2023, **2**, 100075.
16 H. A. Andreas, *J. Electrochem. Soc.*, 2015, **162**, A5047–A5053.
17 J. Niu, B. E. Conway and W. G. Pell, *J. Power Sources*, 2004, **135**, 332–343.
18 X. Yan, Q. Guo, W. Huang, Y. Xiong, S. Jing, X. Zhang, F. Huang and X. Ge, *Carbon Neutralization*, 2023, **2**, 300–309.
19 K. Liu, C. Yu, W. Guo, L. Ni, J. Yu, Y. Xie, Z. Wang, Y. Ren and J. Qiu, *J. Energy Chem.*, 2021, **58**, 94–109.
20 C. Zhong, Y. Deng, W. Hu, J. Qiao, L. Zhang and J. Zhang, *Chem. Soc. Rev.*, 2015, **44**, 7484–7539.
21 A. González, E. Goikolea, J. A. Barrena and R. Mysyk, *Renewable Sustainable Energy Rev.*, 2016, **58**, 1189–1206.
22 B. Pal, S. Yang, S. Ramesh, V. Thangadurai and R. Jose, *Nanoscale Adv.*, 2019, **1**, 3807–3835.
23 M. Zhong, Q. F. Tang, Y. W. Zhu, X. Y. Chen and Z. J. Zhang, *J. Power Sources*, 2020, **452**, 227847.
24 F. Beguin, V. Presser, A. Balducci and E. Frackowiak, *Adv. Mater.*, 2014, **26**, 2219–2251.
25 M. Inagaki, H. Konno and O. Tanaike, *J. Power Sources*, 2010, **195**, 7880–7903.
26 X. Dong and Y. Wang, *Sci. Bull.*, 2020, **65**, 92–93.
27 L. Yin, S. Li, X. Liu and T. Yan, *Sci. China Mater.*, 2019, **62**, 1537–1555.
28 S.-W. Zhang, B.-S. Yin, X.-X. Liu, D.-M. Gu, H. Gong and Z.-B. Wang, *Nano Energy*, 2019, **59**, 41–49.
29 J. Menzel, E. Frąckowiak and K. Fic, *Electrochim. Acta*, 2020, **332**, 135435.
30 A. P. Abbott, G. Capper, D. L. Davies, R. K. Rasheed and V. Tambyrajah, *Chem. Commun.*, 2003, 70–71.
31 Q. Zhang, K. De Oliveira Vigier, S. Royer and F. Jerome, *Chem. Soc. Rev.*, 2012, **41**, 7108–7146.
32 A. P. Abbott, D. Boothby, G. Capper, D. L. Davies and R. K. Rasheed, *J. Am. Chem. Soc.*, 2004, **126**, 9142–9147.
33 J.-L. Yang, X.-X. Zhao, M.-Y. Ma, Y. Liu, J.-P. Zhang and X.-L. Wu, *Carbon Neutralization*, 2022, **1**, 247–266.
34 K. T. T. Tran, L. T. M. Le, A. L. B. Phan, P. H. Tran, T. D. Vo, T. T. T. Truong, N. T. B. Nguyen, A. Garg, P. M. L. Le and M. V. Tran, *J. Mol. Liq.*, 2020, **320**, 114495.
35 Y.-J. Ju, C.-H. Lien, K.-H. Chang, C.-C. Hu and D. S.-H. Wong, *J. Chin. Chem. Soc.*, 2012, **59**, 1280–1287.
36 X. Bu, Y. Zhang, Y. Sun, L. Su, J. Meng, X. Lu and X. Yan, *J. Energy Chem.*, 2020, **49**, 198–204.

37 J. Wu, Q. Liang, X. Yu, Q. F. Lü, L. Ma, X. Qin, G. Chen and B. Li, *Adv. Funct. Mater.*, 2021, **31**, 2011102.

38 R. Puttaswamy, C. Mondal, D. Mondal and D. Ghosh, *SM&T*, 2022, **33**, e00477.

39 T. Li, Y. Xiong, X. Yan, T. Hu, S. Jing, Z. Wang and X. Ge, *J. Energy Chem.*, 2022, **72**, 532–538.

40 F. Huang, T. Li, X. Yan, Y. Xiong, X. Zhang, S. Lu, N. An, W. Huang, Q. Guo and X. Ge, *ACS Omega*, 2022, **7**, 11452–11459.

41 T. El Achkar, H. Greige-Gerges and S. Fourmentin, *Environ. Chem. Lett.*, 2021, **19**, 3397–3408.

42 C. Florindo, F. S. Oliveira, L. P. N. Rebelo, A. M. Fernandes and I. M. Marrucho, *ACS Sustainable Chem. Eng.*, 2014, **2**, 2416–2425.

43 A. P. Abbott, *Curr. Opin. Green Sustainable Chem.*, 2022, **36**, 100649.

44 E. L. Smith, A. P. Abbott and K. S. Ryder, *Chem. Rev.*, 2014, **114**, 11060–11082.

45 B. B. Hansen, S. Spittle, B. Chen, D. Poe, Y. Zhang, J. M. Klein, A. Horton, L. Adhikari, T. Zelovich, B. W. Doherty, B. Gurkan, E. J. Maginn, A. Ragauskas, M. Dadmun, T. A. Zawodzinski, G. A. Baker, M. E. Tuckerman, R. F. Savinell and J. R. Sangoro, *Chem. Rev.*, 2021, **121**, 1232–1285.

46 R. L. McCreery, *Chem. Rev.*, 2008, **108**, 2646–2687.

47 M. Zhong, Q. F. Tang, Z. G. Qiu, W. P. Wang, X. Y. Chen and Z. J. Zhang, *J. Energy Storage*, 2020, **32**, 101904.

48 Y. Wang, Y. Song and Y. Xia, *Chem. Soc. Rev.*, 2016, **45**, 5925–5950.

49 R. L. McCreery, *Chem. Rev.*, 2008, **108**, 2646–2687.

50 H. Wang, S. Liu, Y. Zhao, J. Wang and Z. Yu, *ACS Sustainable Chem. Eng.*, 2019, **7**, 7760–7767.

51 X. Li, L. Liu and H. B. Schlegel, *J. Am. Chem. Soc.*, 2002, **124**, 9639–9647.

52 P. Hobza and Z. Havlas, *Chem. Rev.*, 2000, **100**, 4253–4264.

53 S. Zhu, H. Li, W. Zhu, W. Jiang, C. Wang, P. Wu, Q. Zhang and H. Li, *J. Mol. Graphics Modell.*, 2016, **68**, 158–175.

54 J. Kowal, E. Avaroglu, F. Chamekh, A. Šenfelds, T. Thien, D. Wijaya and D. U. Sauer, *J. Power Sources*, 2011, **196**, 573–579.

55 J. Zhao, J. Zhang, W. Yang, B. Chen, Z. Zhao, H. Qiu, S. Dong, X. Zhou, G. Cui and L. Chen, *Nano Energy*, 2019, **57**, 625–634.

56 A. Y. M. Al-Murshedi, H. F. Alesary and R. Al-Hadrawi, *J. Phys.: Conf. Ser.*, 2019, **1294**, 052041.

57 L. Sapir and D. Harries, *J. Chem. Theory Comput.*, 2020, **16**, 3335–3342.

58 C. Ma, A. Laaksonen, C. Liu, X. Lu and X. Ji, *Chem. Soc. Rev.*, 2018, **47**, 8685–8720.

59 S. Rozas, C. Benito, R. Alcalde, M. Atilhan and S. Aparicio, *J. Mol. Liq.*, 2021, **344**, 117717.

60 S. I. Fletcher, F. B. Sillars, R. C. Carter, A. J. Cruden, M. Mirzaeian, N. E. Hudson, J. A. Parkinson and P. J. Hall, *J. Power Sources*, 2010, **195**, 7484–7488.

61 T. Zhekenov, N. Toksanbayev, Z. Kazakbayeva, D. Shah and F. S. Mjalli, *Fluid Phase Equilib.*, 2017, **441**, 43–48.

62 A. Yadav and S. Pandey, *J. Chem. Eng. Data*, 2014, **59**, 2221–2229.